Journal of Oil Palm Research Vol. 29 (1) March 2017 p. 97 – 109

CORROSION INHIBITION OF MILD STEEL IN HYDROCHLORIC ACID SOLUTION USING FATTY ACID DERIVATIVES

MOHD, N K*; MARIYAM JAMEELAH GHAZALI; YEONG SHOOT KIAN*; NOR AZOWA IBRAHIM‡; WAN MD ZIN WAN YUNUS‡‡; SITI MARIAM MOHD NOR‡ and ZAINAB IDRIS***

ABSTRACT

The inhibitive actions of fatty acid derivatives namely palmitate hydrazide (PH), N-ethylidene palmitate hydrazide (EPH) and N-phenylmethylidene palmitate hydrazide (PPH) on mild steel in 1 M hydrochloric acid were investigated using open circuit potential, linear polarisation and electrochemical impedance spectroscopy techniques. It was observed that the percentage of inhibition efficiency (η%) increased with increasing concentrations of inhibitor and temperature of test medium. The maximum η% approaches 85% in the presence of 200 mg litre^{-1} of inhibitors EPH and PPH at 308 ± 1K. The inhibitor efficiencies were found to be in the following order: PPH>EPH>PH. The adsorption of these inhibitors on mild steel surface obeys Langmuir adsorption isotherm. They act as mixed-type inhibitors. Scanning electron microscopy-energy dispersive X-ray (SEM-EDX) was also carried out on polished mild steel coupons and those immersed in the test medium with the absence and presence of 200 mg litre^{-1} of the inhibitors studied.

Keywords: corrosion inhibition, fatty acid derivatives, Schiff base, mild steel.

Date received: 5 September 2016; **Sent for revision:** 5 September 2016; **Received in final form:** 7 November 2016; **Accepted:** 18 November 2016.

INTRODUCTION

Organic inhibitors which contain heteroatoms like nitrogen, sulphur and oxygen atoms; and/or multiple bonds in their structures are reported exhibiting corrosion inhibition properties toward metals in acidic media. These inhibitors have been thoroughly investigated in developing green and efficient corrosion inhibitors. Organic inhibitors are prepared from chemical synthesis and some are directly obtained from plants through extraction (Raja and Sethuraman, 2008). Theoretically, the adsorption of organic inhibitors on metal surfaces occurs through the displacement of water molecules on the corroding surface followed by the formation of a barrier (El-Maksoud, 2008) as shown by Equation (1). This process results in a reduction of anodic reaction or cathodic reaction or both thus decreasing the corrosion rate.

$$[\text{Inhibitor}]_{sol} + [n\text{H}_2\text{O}]_{ads} \longrightarrow [\text{Inhibitor}]_{ads} + [n\text{H}_2\text{O}]_{sol} \quad \text{Equation (1)}$$

where n is the number of water molecules displaced by an inhibitor molecule.

Recently, Schiff bases have received considerable attention as they could provide greater inhibition through adsorption compared to their respective amine or carbonyl compounds. Such behaviour is basically correlated with the presence of lone pair of electrons on the nitrogen at imine (C=N). The lone pair of electrons are available to be

* Malaysian Palm Oil Board, 6 Persiaran Institusi, Bandar Baru Bangi, 43000 Kajang, Selangor, Malaysia.
E-mail: noorkhairin@mpob.gov.my

** Department of Electrical Engineering, Universiti Kebangsaan Malaysia, 43600 Bangi, Selangor, Malaysia.

‡ Department of Chemistry, Universiti Putra Malaysia, 43400 UPM Serdang, Selangor, Malaysia.

‡‡ Department of Chemistry, National Defence University of Malaysia, Sungai Besi Camp, 57000 Kuala Lumpur, Malaysia.

shared with metals to form a dative covalent bond and a barrier to corrosive species attack (Keles *et al*., 2015). In addition, the inhibitive action of Schiff bases is also attributed to the unoccupied π-orbitals that allow a donation of electrons from the metal *d*-orbitals to the inhibitors (Hosseini *et al*., 2003; Desai *et al*., 1986; Madkour and Elroby, 2014).

The development of nitrogenous compounds containing long alkyl chains (*e.g.* C_8-C_{18}) such as fatty amide (Alam *et al*., 2009), imidazoline (Chen *et al*., 2000; Miksic *et al*., 2006), thiosemicarbazide (Quraishi *et al*., 2000), hydrazide (Quraishi *et al*., 2000), ethoxylated fatty alkyl amine (Migahed *et al*., 2006), nitrile (Palou *et al*., 2014), dihydroxystearic acid (Roila *et al*., 2001) and quarternary ester (Monk, 2015) as corrosion inhibitors was a recent discovery. These compounds are basically derived from vegetable oils. They consist of a polar head and a hydrophobic tail. In the aqueous test solution, the polar head interacts with the metal surfaces forming a barrier. The hydrophobic group on the other hand tends to move away from the metallic surface forming a hydrophobic layer. The hydrophobic layer provides an additional protection against corrosive species (Chen *et al*., 2000; Miksic *et al*., 2009; Negm *et al*., 2011; Tiu and Advincula, 2015).

The study of the potential of palmitate hydrazide (PH) and Schiff base compounds namely N-ethylidene palmitate hydrazide (EPH) and N-phenylmethylidene palmitate hydrazide (PPH) as corrosion inhibitors (*Table 1*) is limited and not well-known. The presence of heteroatoms, π-electrons and long alkyl chain (C16) in their molecular structures is expected to demonstrate high inhibition efficiency toward metallic surfaces. This article documents the study on the inhibition effect of these inhibitors on mild steel (MS) in 1 M HCl using linear polarisation (LP) and electrochemical impedance spectroscopy (EIS). The inhibition action of these compounds was further confirmed by scanning electron microscopic analysis (SEM) of the MS coupon in the presence or absence of the inhibitors. The development and utilisation of these palmitic acid derivatives could add value to palm oil as palmitic acid is one of the major components of palm oil (Tarmizi *et al*., 2008).

MATERIALS AND METHODS

Materials

Hydrazine monohydrate with a purity of 60%-64% was obtained from Merck (Germany). Propionaldehyde and benzaldehyde used were purchased from Sigma-Aldrich (USA) and methyl hexadecanoate with purity of >95% was obtained from Acros Organic (USA). All other reagents were of analytical grade and used as received. Inhibitors of PH, EPH and PPH were synthesised and purified in the laboratory.

Synthesis of PH

A mixture of methyl hexadecanoate (74.01 g, 0.27 mol), hydrazine monohydrate (50.39 g, 0.60 mol) and absolute ethanol (150 ml) was poured into a 500-ml round bottom flask. The reaction mixture was constantly stirred under reflux system at 78°C for 3 hr. The resulting solution was cooled at ambient temperature and left overnight. Subsequently, the solution was filtered under reduced pressure to retain the white precipitate. Recrystallisation from ethanol was performed followed by drying in oven at 50°C-60°C. Appropriate precautions were strictly taken when handling, storing and disposing hydrazine monohydrate.

PH. White flakes (93%); *m.p.*: 111.5°C-112.5°C; ϑ_{max} (KBr) 3321 (N-H primary amine), 3290 (N-H primary amine), 3180 (N-H), 1633 (C=O), 1538 (N-H), 1161 (C-N), 719 (N-H) cm^{-1}; δ_H (500 MHz, $CDCl_3$) 6.67 (s, 1H, CONH), 3.90 (br.*s*, 2H, NH_2), 2.13 (t, 2H, *J* 8.00 Hz, CH_2CO), 1.62 (m, 2H, CH_2CH_2CO), 1.28 (m, 24H, $(CH_2)_{12}CH_3$), 0.87 (t, 3H, *J* 6.90 Hz, CH_2CH_3);

TABLE 1. CHEMICAL STRUCTURES AND PHYSICO-CHEMICAL PROPERTIES

Chemical name	Chemical structure	Physical appearance	*m.p.*(°C)	Purity (%)	Yield (%)
PH	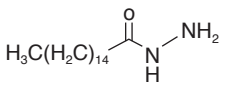	White flakes	112.4	>96	93
EPH	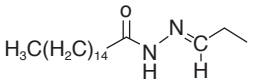	White powder	86.6	>96	98
PPH	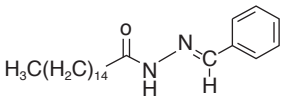	White powder	88.1	>96	99

Note: PH - palmitate hydrazide.
EPH - *N*-ethylidene palmitate hydrazide.
PPH - *N*-phenylmethylidene palmitate hydrazide.
m.p. - melting point.

δ_C (125 MHz, $CDCl_3$) 174.1 (<u>C</u>O), 34.7 (<u>C</u>H_2CO), 32.0 (<u>C</u>H_2CH_2CO), 29.55 (<u>C</u>$H_2)_{10}$, 29.4 (<u>C</u>$H_2CH_2CH_3$), 29.3 (<u>C</u>H_2CH_3), 14.1 (CH_2<u>C</u>H_3); *m/z* (EIMS): 399 [(M-C_7H_{15})$^+$, $C_{18}H_{43}N_2OSi_3$]; CHN analysis (%) C: 72.18, H: 12.42, N: 12.78; calculated ($C_{16}H_{34}N_2O$): C: 71.11, H: 12.59, N: 10.37.

Synthesis of EPH and PPH

A solution of PH (2.70 g, 0.01 mol) in dimethylformamide (20 ml) was mixed with the solution of corresponding aldehydes (propionaldehyde and benzaldehyde, 0.05 mmol) in a two-necked round bottom flask. Reaction mixture was heated and constantly stirred for approximately 2 hr. After the completion of the reaction, distilled water (5 ml) was added into the resulting solution to give a white precipitate. Subsequently, the white precipitate was collected and recrystallised from dimethylformamide and water. The weight of the corresponding precipitate was recorded.

EPH. White powder (98%); *m.p.*: 86.6°C-85.9°C; TLC (silica): R_f = 0.25 (eluent: petroleum ether-ethyl acetate, 8:2, *v/v*); ϑ_{max} (KBr) 3211 (N-H), 1664 (C=O), 1630 (C=N), 1557 (N-H), 1188 (C-N), 719 (N-H) cm^{-1}; δ_H (500 MHz, $CDCl_3$) 9.58 (br.s, 1H, CON<u>H</u>), 7.18 (t, 1H, *J* 4.60 Hz, N=C<u>H</u>), 2.60 (t, 2H, *J* 8.00 Hz, C<u>H</u>$_2$CO), 2.25 (m, 2H, NCHC<u>H</u>$_2$CH$_3$), 1.63 (m, 2H, C<u>H</u>$_2$CH$_2$CO), 1.23 [m, 24H, (C<u>H</u>$_2$)$_{12}$CH$_3$], 1.10 (t, 3H, *J* 8.00 Hz, NCHCH$_2$C<u>H</u>$_3$), 0.87 (t, 3H, *J* 8.05 Hz, CH$_2$C<u>H</u>$_3$); δ_C (125 MHz, $CDCl_3$) 176.3 (<u>C</u>O), 148.2 (N<u>C</u>H), 32.7 (<u>C</u>H_2CO), 32.0 (<u>C</u>H_2CH_2CO), 29.7 (<u>C</u>$H_2)_{10}$, 25.6 (CH_2<u>C</u>H_2CH_3), 24.8 (<u>C</u>$H_2CH_2CH_3$), 22.8 (<u>C</u>H_2CH_3), 14.2 (CH_2<u>C</u>H_3), 10.6 (NCHCH$_2$<u>C</u>H$_3$); *m/z* (EIMS): 382 (M$^+$, C_{22}H46N_2OSi); CHN analysis (%) C: 74.02, H: 12.51, N: 10.23; calculated ($C_{17}H_{34}N_2O$): C: 73.55, H: 12.26, N: 9.03.

PPH. White powder (99%); *m.p.*: 88.1°C-87.7°C; TLC (silica): R_f = 0.36 (eluent: petroleum ether-ethyl acetate, 8:2, *v/v*); ϑ_{max} (KBr) 3188 (N-H), 1671 (C=O), 1604 (C=N), 1651 (C=C), 1557 (N-H), 1186 (C-N), 722 (N-H) cm^{-1}; δ_H (500 MHz, $CDCl_3$) 9.72 (br., 1H, CON<u>H</u>), 7.79 (s, 1H, N=C<u>H</u>), 7.66 (t, 2H, *J* 4.55 Hz, <u>*m*-phenyl</u>), 7.39 (m, 3H, <u>*o*-phenyl</u> and <u>*p*-phenyl</u>), 2.76 (t, 2H, *J* 8.05 Hz, C<u>H</u>$_2$CO), 1.73 (m, 2H, C<u>H</u>$_2$CH$_2$CO), 1.26 (m, 24H, (C<u>H</u>$_2$)$_{12}$CH$_3$), 0.87 (t, 3H, *J* 6.90 Hz, CH$_2$C<u>H</u>$_3$); δ_C (125 MHz, $CDCl_3$) 176.7 (<u>C</u>O), 143.4 (N=<u>C</u>H), 134.0 (1C, <u>phenyl</u>), 130.2 (1C, <u>phenyl</u>), 128.8 (2C, <u>phenyl</u>), 127.2 (2C, <u>phenyl</u>), 32.9 (CH_2CO), 32.0 (<u>C</u>H_2CH_2CO), 29.7 ($CH_2)_{10}$, 24.9 (<u>C</u>$H_2CH_2CH_3$), 22.8 (<u>C</u>H_2CH_3), 14.2 (<u>C</u>H$_3$); *m/z* (EIMS): 430 (M$^+$, $C_{26}H_{46}N_2OSi$); CHN analysis (%) C: 76.37, H: 9.63, N: 8.21; calculated ($C_{17}H_{34}N_2O$): C: 77.09, H: 10.61, N: 7.82.

The methodology for preparing EPH and PPH inhibitors was also published in Malaysian patent application PI 2014003628 (Mohd *et al*., 2014).

Test Solution

Analytical grade 37% HCl was diluted with ultra-pure water (resistivity > 18 MΩ cm) to prepare 1 M HCl. A stock solution containing 2500 mg litre^{-1} inhibitor in an alcohol was diluted appropriately with 1 M HCl solution to obtain various concentrations: 25-200 mg litre^{-1}. All test solutions were freshly prepared before each experiment.

Mild Steel Coupons

Mild steel (MS) coupons (2.5 cm × 2.5 cm × 0.3 mm) were mechanically abraded with 80, 150, 250, 400, 1500 grade emery papers to obtain a mirror-like surface and free from apparent defects. The coupons were washed with distilled water, degreased with acetone, dried in an oven at 60°C-70°C for 1 hr and kept in a desiccator.

Corrosion Measurement

The inhibition properties were investigated via electrochemical techniques using a Methrom potentiostat (PG104, Netherland) equipped with a 100-ml water-jacketed corrosion cell and a three electrode cell assembly. The electrode cell assembly consists of MS coupon with an exposed area of 4.53 cm^2 as a working electrode (WE), a platinum counter electrode (CE), an Ag/AgCl in 3 M KCl as a reference electrode (RE) and an earth connection. The potentiostat was controlled by NOVA 1.10 software and measurement was carried out under non-stirred condition. Before performing each test, the WE was immersed in the test solution until a steady state potential was attained. The steady state signifies oxidation current (I_{ox}) is equal to reduction current (I_{red}) or in equilibrium state.

Scanning Electron Microscopy- Energy Dispersive X-ray (SEM-EDX) Analysis

The surface morphology of MS coupon was examined using scanning electron microscopy (JEOL 840 SEM, Japan) attached to the energy dispersive X-ray analysis (Oxford INCA400) (Oxford Instrument Analytical, Bucks, United Kingdom). Polished MS coupons were immersed in the test solutions containing 200 mg litre^{-1} inhibitor at room temperature for 30 days. The MS coupons were washed with distilled water, dried in a desiccator before examining the surface.

RESULTS AND DISCUSSION

Open Circuit Potential Measurements

The variation of the open circuit potential (OCP) *vs*. Ag/AgCl in 3 M KCl with time for MS

in the test solution containing inhibitor and without inhibitor (blank) is presented in *Figure 1*. It is clear from the curves that the corrosion potentials of MS in inhibited and uninhibited 1 M HCl give negative values. The corrosion potential of MS in the blank solution decreases steadily with time towards more negative values. This condition was due to a breakdown of the pre-immersion air formed iron oxide (Fe_2O_3) film that was present on the MS surface according to Equation (2) (Migahed *et al*., 2006).

$$Fe_2O_3 + 6HCl \rightarrow 2FeCl_3 + 3H_2O \qquad \text{Equation (2)}$$

Then, a new iron oxide film grew inside the test solution causing the potential shifted again to a more noble direction until the steady state potential obtained. The potential values of the blank solution are in the range of -0.451 V and -0.458 V, within 800 s. The curves become more stable with the increasing of exposure time. In contrast, the addition of inhibitors in 1 M HCl resulted in negative shifts of OCP values. The negative shift could be related to cathodic reaction that was obstructed by the inhibitors.

Linear Polarisation Measurements

The cathodic and anodic polarisation curves of the MS coupons immersed in uninhibited and inhibited 1 M HCl (*Figure 2*) were obtained by scanning the corrosion potential (E_{corr}) at a scan rate of 1 mV s^{-1}. The addition of PH, EPH and PPH has modified slightly both the anodic and cathodic slopes indicating that the inhibitors had reduced the anodic dissolution and retard the hydrogen evolution process. These findings are in accordance with the study done by Negm *et al*. (2011). The changes in slopes for both anode and cathode signify a mixed-type of inhibitor behaviour (Bentiss *et al*., 2009). It is also noted that the anodic Tafel slopes decrease proportionally to the amount of inhibitors. This could be attributed to the better surface coverage that was achieved at the higher loading of inhibitor. Once the inhibitors get adsorbed on the MS surface, they retard both anodic and cathodic reactions, which successively reduced the surface area for the subsequent surface reactions. The presence of inhibitors also results in a shifts of cathodic curves towards lower current density (log *I*) values. The shift of the cathodic curves is more significant when the inhibitor concentration is increased. Basically, this behaviour reveals that the inhibitors exhibit inhibition activities. The Tafel parameters of corrosion potential (E_{corr}), corrosion current (i_{corr}), anodic slope (β_a), cathodic slope (β_c), corrosion rate (CR) and inhibition efficiency ($\eta\%$) for MS coupons in 1 M HCl in the presence of different concentration of PH, EPH and PPH as inhibitors at 308 ± 1 K are presented in *Table 2*. The inhibition efficiencies were determined using Equation (3);

$$\text{Inhibition efficiency, } \eta\% = \frac{i_{corr} - i'_{corr}}{i_{corr}} \times 100 \qquad \text{Equation (3)}$$

where i_{corr} and i'_{corr} are the corrosion currents in the absence and presence of inhibitor, respectively. In the absence of inhibitor, the i_{corr} and CR values are found to be at 289.48 μA cm^{-2} and 3.36 mm yr^{-1}, respectively. The MS coupon undergoes active metal dissolution process at the anode and hydrogen evolution process at the cathode. However, an addition of 25 mg $litre^{-1}$ inhibitor in the test solution results in a marked reduction of i_{corr} and CR values to less than

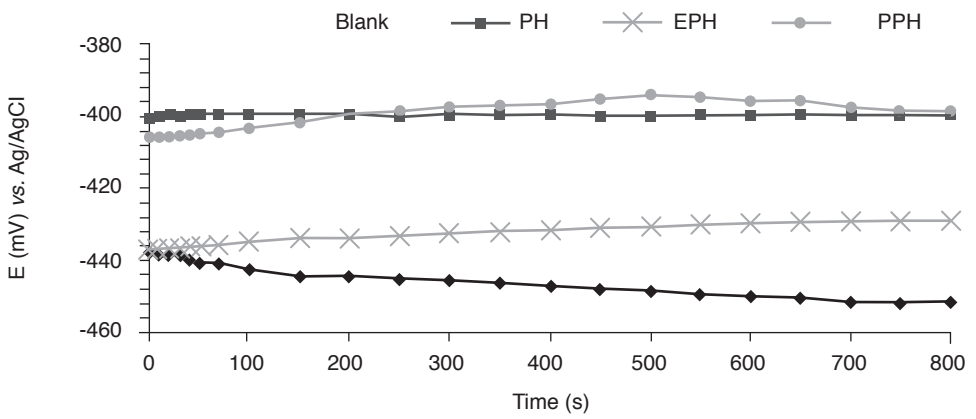

Note: PH - palmitate hydrazide.
EPH - *N*-ethylidene palmitate hydrazide.
PPH - N-phenylmethylidene palmitate hydrazide.

Figure 1. Open circuit potential curves of the mild steel in 1 M HCl in the absence and presence of 200 mg litre^{-1} inhibitor as a function of exposure time at 308 ± 1 K.

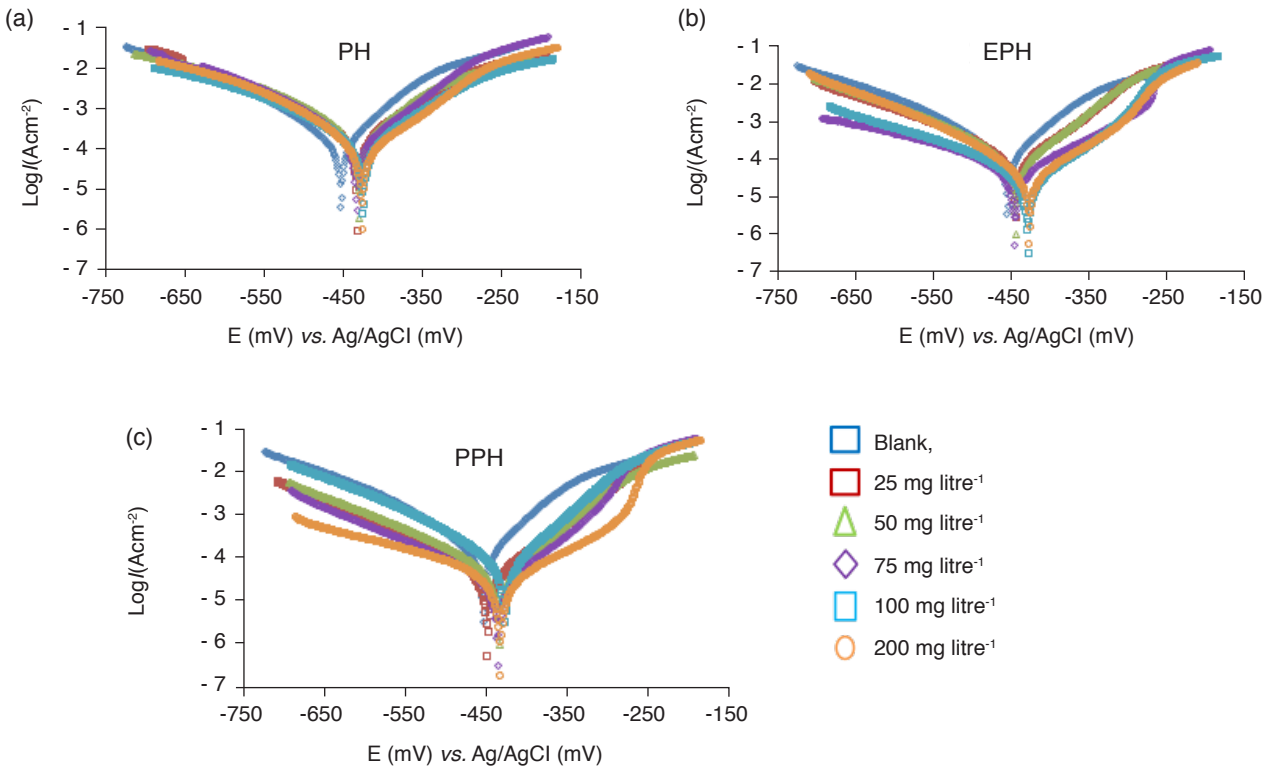

Figure 2. Tafel polarisation curves of mild steel coupons after immersion in 1 M HCl in the presence of 25, 50, 75, 100 and 200 mg litre^{-1} of (a) palmitate hydrazide (PH), (b) N-ethylidene palmitate hydrazide (EPH) and (c) N-phenylmethylidene palmitate hydrazide (PPH) at 308 ± 1K

TABLE 2. TAFEL POLARISATION PARAMETERS FOR MILD STEEL IN 1 M HCl WITH DIFFERENT CONCENTRATIONS OF PH, EPH AND PPH AT 308 + 1 K

	Concentration (mg litre^{-1})	$-E_{corr}$ (mV *vs.* Ag/AgCl)	i_{corr} (μA cm^{-2})	CR (mm yr^{-1})	Inhibition efficiency (η%)
Blank	-	-452	289.48	3.36	-
PH	25	-453	85.94	1.00	70.3
	50	-451	74.79	0.87	74.2
	75	-433	71.23	0.83	75.4
	100	-426	56.34	0.66	80.5
	200	-416	14.60	0.17	80.3
EPH	25	-443	102.51	1.19	64.6
	50	-443	85.91	1.00	70.3
	75	-465	72.38	0.84	75.0
	100	-428	53.05	0.62	81.7
	200	-442	42.40	0.49	85.4
PPH	25	-436	82.87	0.96	71.4
	50	-434	71.06	0.83	75.5
	75	-448	59.02	0.69	79.6
	100	-426	55.56	0.65	80.8
	200	-433	44.81	0.52	84.5

Note: PH - palmitate hydrazide.
EPH - *N*-ethylidene palmitate hydrazide.
PPH - *N*-phenylmethylidene palmitate hydrazide.

102.51 μA cm^{-2} and 1.19 mm yr^{-1}, respectively. This implies that the inhibitors gradually retard both the anodic and cathodic processes. Further increase in inhibition concentration results in more interaction between inhibitor and metal surface thus reducing the surface area for subsequent reactions. This leads to decreases in CR and i_{corr} values thereby increasing η% value.

Apart from it, the E_{corr} values have shifted toward more positive direction with reference to the blank solution suggesting that the suppression of the anodic reaction is the pre-dominant effect.

The shift in E_{corr} values is more significant at higher inhibitor concentrations. It was suggested that, if the shift in E_{corr} values is > 85 mV in inhibited solution with reference to uninhibited solution, the inhibitors could be classified as cathodic or anodic type depending on its direction. But, if the shift in E_{corr} values is < 85 mV, the inhibitors could be recognised as mixed-type inhibitors (Verma and Quraishi, 2014). In this study, the changes in E_{corr} values are less than 85 mV indicating they act as a mixed-type inhibitor.

At constant temperature, the η% values of all inhibited solutions increase with increasing inhibitor concentration (*Figure 3a*). The incorporation of PPH and EPH in 1 M HCl gives the η% values of approximately 85% which are higher than that of PH. It is also noted that the η% values of all studied inhibitors are relatively low at 308 ± 1 K and they steadily increase reaching 95% at 328 ± 1 K (*Figure 3b*). Theoretically, corrosion rate is strongly affected by temperature. An increase of each 10°C may double the corrosion rate (Davis, 2000). Conversely, it was observed that the inhibition efficiencies strongly increase with increasing temperature. These results could be associated with the solubility of the inhibitors in the test medium. It is greater at higher temperature thus giving higher η% values. The η% values increase in the following order PPH > EPH > PH. The inhibition behaviour of EPH and PPH could be correlated to the presence of imine in their molecule structures that enables a strong adsorption with the metal surface, hence, providing better inhibition. PPH shows better inhibition properties than EPH because it has a phenyl group that allows the adsorption of delocalised π-electrons with the vacant *d*-orbital of Fe atom (Madkour and Elroby, 2015).

Electrochemical Impedance Spectroscopy Measurement

The EIS results are interpreted in term of the equivalent circuit of the double layer resulting from the charge transfer resistance, R_{ct}, solution resistance, R_s and capacitance double layer, C_{dl} (*Figure 4*). The circuit is commonly used to model the metal-electrolyte interface. A constant phase element (CPE) is used to describe a frequency of independent phase shift between an applied attenuated current potential and its current response as in Equation (4)

$$Z(CPE) = Y_o^{-1} (j\omega)^{-n} \qquad \text{Equation (4)}$$

where $j = \sqrt{(-1)}$, ω is the angular frequency in rads^{-1}, Y_o is the constant of CPE element, n is an empirical constant that ranges from 0 to 1. When $n = 1$, the CPE performs as a pure capacitor, if $n = 0$, the CPE behaves as a pure resistor and if $n = 0.5$, the CPE is an equivalent of the Warburg element. Warburg element is a diffusion of ohmic species at the interface. The exponent of the CPE element which can be used as a gauge for the heterogeneity or roughness of the surface and f is the frequency of sinusoidal perturbation signal in Hz. Conversion of fit parameter Y_o into C_{dl} can be done through the following relationship as shown in Equation (5):

$$C_{dl} = \frac{1}{(2\pi f_{max} R_{ct})} \qquad \text{Equation (5)}$$

where f is the frequency at which the imaginary component of the impedance is at a maximum while R_{ct} values, obtained from the parametric fit of the experimental spectrum to the equivalent circuit equation. The impedance spectra (Nyquist plots) for PH, EPH and PPH (*Figure 5*) as well as uninhibited

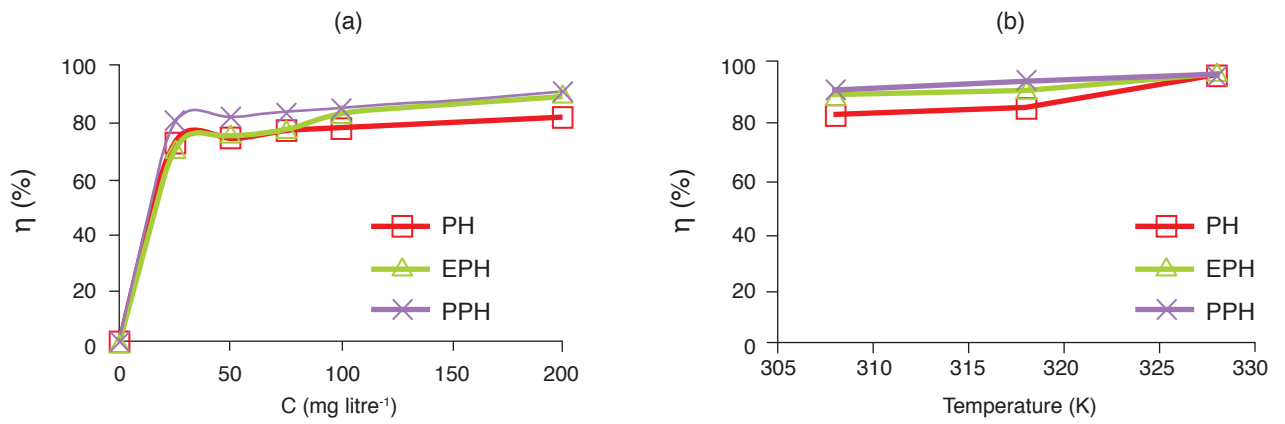

Note: PH - palmitate hydrazide.
EPH- *N*-ethylidene palmitate hydrazide.
PPH- *N*-phenylmethylidene palmitate hydrazide.

Figure 3. The effects of inhibitor concentration at 308 ± 1 K (a) and temperature at 200 mg litre^{-1} inhibitor (b) on the inhibitor efficiency of mild steel in 1 M HCl.

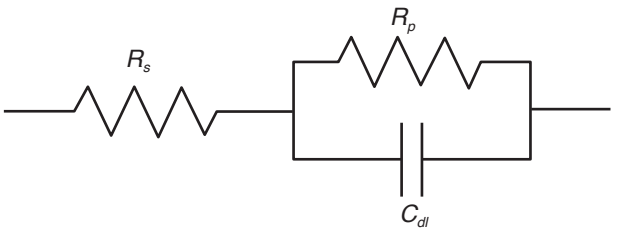

Figure 4. An electrochemical equivalent circuit diagram for metal-electrolyte interface.

solution appeared as single semi-circle capacitive loops suggesting that the corrosion process is mainly controlled by a charge transfer process (El-Lateef *et al*., 2015). The smallest capacitive loop was obtained from experiment of MS in uninhibited solution and indicates that, the metal is having an active corrosion process in the test solution. The large capacitive loop is associated with a slower corroding process.

The Nyquist plots of MS in 1 M HCl solution containing the studied inhibitors show imperfect semi-circles. These are often related to a frequency dispersion that are attributed to the roughness of metal surface, impurities, dislocations and formation of porous layers (Ramya *et al*., 2015; Abdulwali *et al*., 2013). It is clearly observed that the shape of the Nyquist plots is not affected by the presence of inhibitor molecules as all plots obtained are single semi-circle capacitive loops. This suggests that the inhibitors do not change the corrosion mechanism of the MS in 1 M HCl and the inhibition occurs through the adsorption on the MS surface (Solmaz *et al*., 2008). It was also observed that the diameters of semi-circles noticeably increase with the addition of inhibitors. The size of capacitive loop increases as a consequence of increasing inhibitor concentrations. The capacitive loops for EPH and PPH are relatively bigger than PH suggesting the corroding process of MS is relatively slower in the presence of these inhibitors. The high-frequency capacitive loops suggest that the corroding process of MS in 1 M HCl is controlled by a charge transfer process (Abdulwali *et al*., 2013; Ashassi-Sorkhabi *et al*., 2006). The low-frequency inductive loops might be attributed to the relaxation process that resulted from adsorption of Cl^-_{ads} and the re-dissolution of the passive surface. The disappearance of inductive loops at high inhibitor concentrations signifies the formation of a protective layer on the metal surface (Khadiri *et al*., 2016). In general, when MS is immersed in inhibited and uninhibited test solutions it behaves like a pure capacitor as the constant, *n* values are very close to one (*Table 3*).

The similar trend on changes of R_{ct} and C_{dl} values were observed by increasing the inhibitor concentration. The R_{ct} value represents a corroding process whereby a high value is associated with a slower corroding system. The rise in R_{ct} values is due to the increase in thickness of the electrical double layer (EDL) that results in better resistance toward charge transfer reactions at the metal-electrolyte interface. The decrease in C_{dl} values is attributed to the adsorption of inhibitor molecules on the metal surface thus preventing the extent of the metal dissolution (Rafiquee *et al*., 2007). Helmholtz model as shown by Equation (6) can be used for further understanding on this phenomenon.

$$C_{dl} = \frac{\varepsilon_o \varepsilon}{d} S \qquad \text{Equation (6)}$$

TABLE 3. CONSTANT PHASE ELEMENT (CPE) OF MILD STEEL IN 1 M HCl WITH DIFFERENT CONCENTRATION OF PH, EPH AND PPH AT 308 ± 1K

Inhibitor	Concentration (mg litre^{-1})	Constant (*n*)	R_s (Ω)	R_{ct} (Ω)	C_{dl} (μF cm^{-2})
Uninhibited (blank)	-	0.999	1.43	103	40.4
	25	0.998	1.40	111	63.5
	50	0.998	1.36	117	62.9
PH	75	0.998	1.39	114	61.5
	100	0.997	1.68	152	61.5
	200	0.996	1.78	345	38.0
	25	0.997	1.20	120	53.1
	50	0.997	1.34	157	53.9
EPH	75	0.997	1.40	176	43.3
	100	0.996	1.41	291	38.4
	200	0.997	1.53	559	37.2
	25	0.998	1.12	211	36.9
	50	0.998	1.59	222	36.1
PPH	75	0.997	2.10	242	37.0
	100	0.997	1.51	289	34.3
	200	0.998	1.51	176	50.7

Note: PH - palmitate hydrazide.
EPH - *N*-ethylidene palmitate hydrazide.
PPH - *N*-phenylmethylidene palmitate hydrazide.

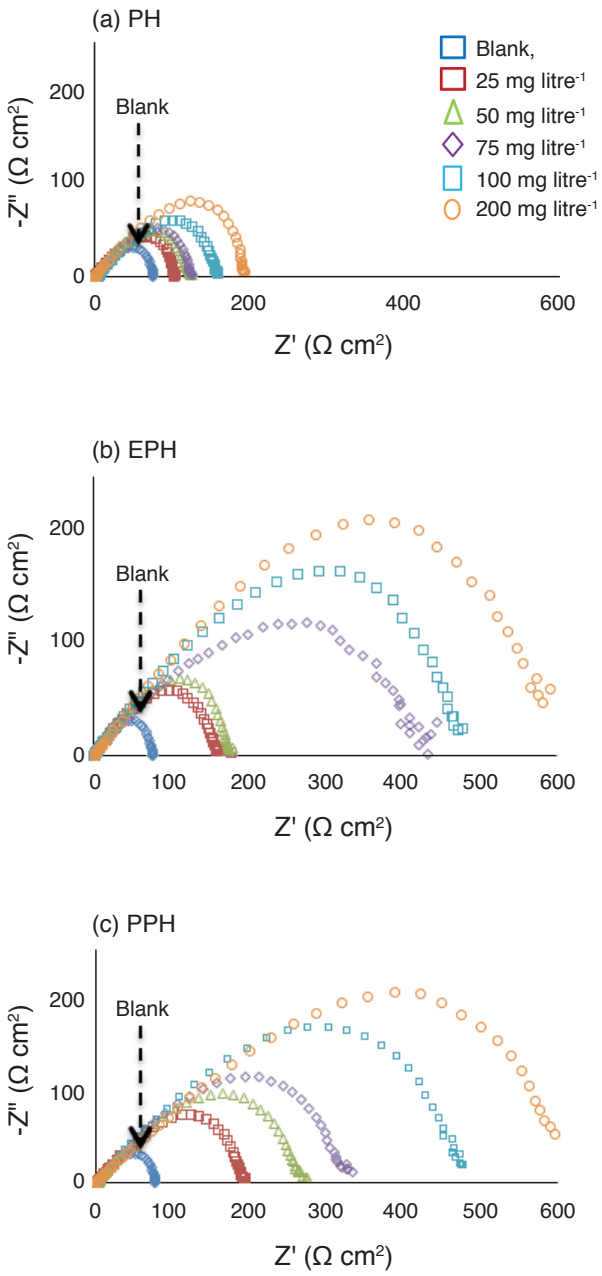

Figure 5. Nyquist plots for mild steel in 1 M HCl with difference concentrations of (a) palmitate hydrazide (PH), (b) N*-ethylidene palmitate hydrazide (EPH) and (c)* N*-phenylmethylidene palmitate hydrazide (PPH) at 308 ± 1K.*

where ε_o is the permittivity of free space, ε is the local dielectric constant of the protective layer, d is the film thickness and S is the surface area. In this model, the C_{dl} is inversely proportional to the surface change. The decrease in C_{dl} might be due to a reduction in local dielectric constant (ε) and/or an increase in the thickness (d) of the EDL at the MS surface. The replacement of water molecules with inhibitor molecules decreases the local dielectric constant as it involves replacement of higher dielectric constant to lower dielectric constant (Özcan *et al*., 2008).

Adsorption Isotherm

The inhibitive action of PH, EPH and PPH on the MS surface is best described by the Langmuir type adsorption. The Langmuir adsorption isotherm, θ is associated with the concentration of the inhibitor as given by Equation (7). This model assumes each adsorption site holds only one adsorbed species (Foo and Hameed, 2010) and inhibitors formed self-assembled monolayers (SAM).

$$\theta = kC/(1 + kC) \qquad \text{Equation (7)}$$

where k is the equilibrium constant of the adsorption process and rearrangement of Equation (7) gives Equation (8):

$$\frac{C_{inh}}{\theta} = \frac{1}{K_{ads}} + C_{inh} \qquad \text{Equation (8)}$$

where C_{inh} is the concentration of inhibitor and K_{ads} is the adsorption constant obtained from the intercept of the straight line. The plots of C_{inh}/θ against C_{inh} (*Figure 6*) gave straight lines with linear regressions, r^2 of > 0.99. The Kads is related to the standard free energy of adsorption (ΔG_{ads}) as described by Equation (9):

$$\Delta G_{ads} = \text{-RT ln}(55.5\ K_{ads}) \qquad \text{Equation (9)}$$

where R is the universal gas constant (R= 8.31446 J K mol^{-1}), T is absolute temperature (K) and the value of 55.5 represents the molar concentration of water in solution expressed in unit of mol litre^{-1} (El-Lateef, 2015). Values of ln K_{ads}, ΔG_{ads} and H_{ads} are shown in *Table 4*. The ln K_{ads} values for all inhibitors are found in the range of 8.53 to 11.26 signifying these inhibitors strongly adsorbed onto the MS surface. The increase in adsorption of inhibitors on MS surface in accordance with temperature is also shown by *ln* K_{ads} values. Apart from having better solubility at higher temperatures giving greater adsorption, it is also hypothesised that the mode of adsorption is also affected by temperature. The inhibitor adsorbs on the metal surface by physisorption at lower temperatures. Adversely, chemisorption is favoured at higher temperatures (Lebrini *et al*., 2006; Bouklah *et al*., 2006; Bentiss *et al*., 2005). The negative values of ΔG_{ads} signify a spontaneity adsorption of the inhibitors on the MS surface (Solmaz *et al*., 2008). Basically, physisorption process is indicated by ΔG_{ads} values of < -20 kJ mol^{-1} as it involves electrostatic interactions between the charged molecules (physisorption). Nevertheless, chemisorption process is associated with ΔG_{ads}values around -40 kJ mol^{-1} or higher as results of sharing or transfer of electrons from organic molecules to metallic surfaces through formation of coordinate

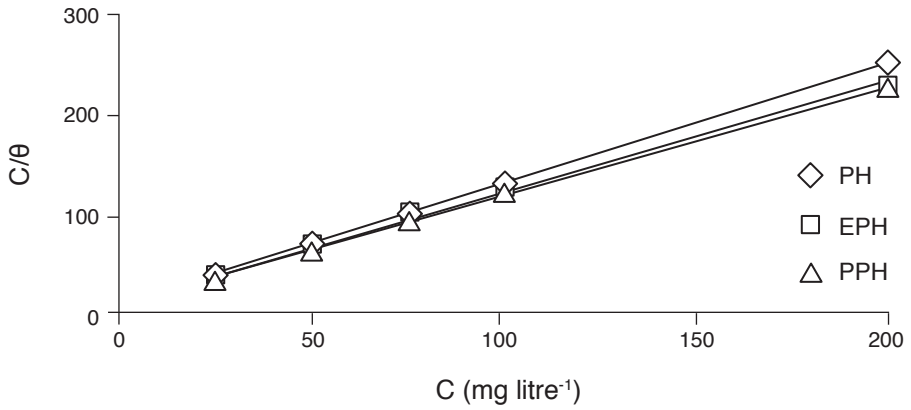

Note: PH - palmitate hydrazide.
EPH - *N*-ethylidene palmitate hydrazide.
PPH - *N*-phenylmethylidene palmitate hydrazide.

Figure 6. Langmuir absorption isotherm of PH, EPH and PPH at 308 ± 1 K.

TABLE 4. LANGMUIR ADSORPTION ISOTHERM PARAMETERS FOR PH, EPH AND PPH ON MILD STEEL SURFACE IN 1 M HCl AT DIFFERENT TEMPERATURES

Inhibitor	Temperature (K)	ln K_{ads} (L mol^{-1})	ΔG_{ads} (kJ mol^{-1})	ΔH_{ads} (kJ mol^{-1})
	298	8.53	-31.1	
	308	9.56	-34.8	-37.2
PH	318	9.88	-36.7	
	328	11.17	-41.4	
	298	9.10	-32.5	
	308	10.01	-35.9	-50.3
EPH	318	11.19	-40.2	
	328	11.21	-41.5	
	298	9.49	-33.5	
	308	10.71	-37.7	-54.0
PPH	318	10.41	-38.2	
	328	11.26	-41.7	

Note: PH - palmitate hydrazide.
EPH - *N*-ethylidene palmitate hydrazide.
PPH - *N*-phenylmethylidene palmitate hydrazide.

bonds (Solmaz *et al.*, 2008; Bahrami and Hosseini, 2012). It is found that the ΔG_{ads} values increase proportionally to the rise of temperature with values from -33.6 kJ mol^{-1} to -42.3 kJ mol^{-1}. This value range is the threshold value of both physisorption and chemisorption. Furthermore, this observation also suggests that the adsorptions of inhibitors are predominantly due to chemisorption accompanied by physisorption. Solmaz *et al*. (2008) also recommended that the physisorption could be the initial stage of adsorption process. The enthalpy of adsorption can be calculated from Gibss-Helmholtz equation as expressed by Equation (10):

$$\Delta G_{ads} = \Delta H_{ads} - T\Delta S_{ads} \qquad \text{Equation (10)}$$

Plot of ΔG_{ads} against T (*Figure 7*) gives the entalphy of adsorption (ΔH_{ads}) and the standard entropy (ΔS_{ads}). The plots show good dependence of ΔG_{ads} on T indicating the adsorption of inhibitors is in good correlation with thermodynamic parameters. Basically, negative value of the entalphy of adsorption (ΔH_{ads}<0) indicates an exothermic process that involves either physisorption or chemisorption. While a positive value (ΔH_{ads} >0) is related to an endothermic process through chemisorption (Durnie *et al.*, 1999). The high values of ΔH_{ads} signify the strong adsorption of inhibitors onto the MS surface. In this study, the values of ΔH_{ads} obtained are all negative suggesting the exothermic behaviour of adsorption. The magnitude of ΔH_{ads} for EPH and PPH is higher than PH indicating stronger adsorption of EPH and PPH.

Scanning Electron Microscope Analysis

The SEM micrographs of a finely polished MS coupon after 30 days of immersion in 1 M HCl (control) are depicted in *Figures 8a* and *8b*. The image of the finely polished MS coupon exhibits relatively smooth surface with some scratch lines that arise during metal polishing. After 30 days of immersion,

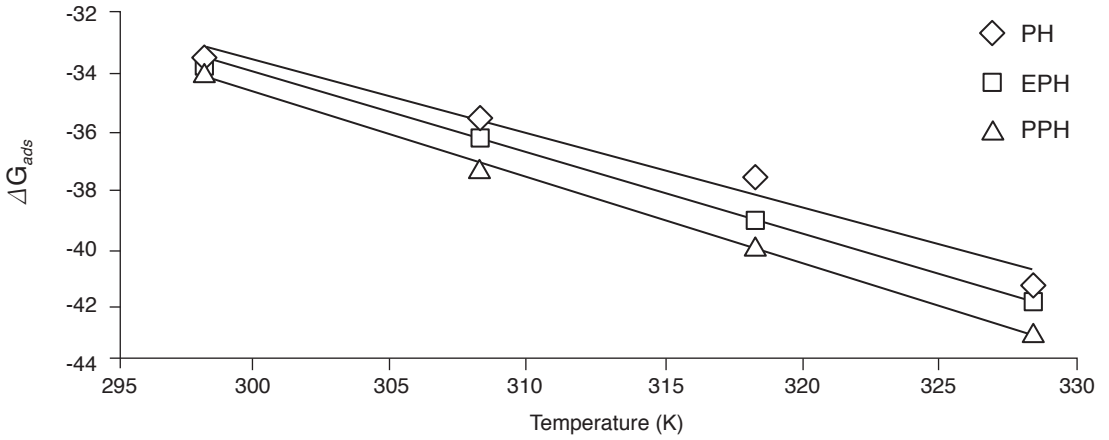

Note: PH - palmitate hydrazide.
EPH - *N*-ethylidene palmitate hydrazide.
PPH - *N*-phenylmethylidene palmitate hydrazide.

Figure 7. Variation of ΔG_{ads} with T (K).

the MS surface suffers severe corrosion. A formation of flakes-type corrosion products resulting from long-term attacks of aggressive corrosive solution is observed in the micrographs. SEM micrograph (*Figure 9a*) of MS coupon after 30 days of immersion in the test solution containing PH shows the surface is very rough with large number of cracks and flakes-type corrosion products. This severe corrosion is almost similar to that of uninhibited (control). The result shows that PH does not able to give sufficient protection toward MS surface for long-term attack of corrosive solution. The micrographs for MS coupons in the test solution containing EPH and PPH (*Figures 9b* and *9c*) exhibit smoother surfaces and the scratch lines are completely invisible signifying the surfaces are covered by a thin protective film. EPH and PPH form protective layers on MS surface thus prevent the surface from attack of corrosive ions, reduce the dissolution process of MS and inhibit the MS surface (El Azzouzi *et al*., 2016). Some deposited particles are also found on the surfaces. This could be due to the multiple nucleations of inhibitors, preferentially on the same site of the MS surface (Karthikaiselvi and Subhashini, 2014).

Energy Dispersive X-ray Analysis

A formation of protective layer on MS surface was also confirmed by analysing the chemical content after 30 days of immersion in the test solution. The EDAX analysis on finely surface MS shows an absence of chlorine and oxygen particles indicating the MS surface is absolutely free from any oxide layer and/or corroded particles. Significant increases in chlorine and oxygen contents are observed for MS coupons that were exposed to uninhibited 1 M HCl solution. The increases in chlorine and oxygen contents could be associated with the formations of $FeCl_2$, $Fe(OH)_2$, Fe_2O_3 and/or Fe_3O_4. The MS surface does not have any protective layer so that it is having severe attack of aggressive corrosive ions forming corroded particles. Addition of 200 mg litre^{-1} PH in the test solution resulted in a decrease in Cl content and an increase in oxygen content signify insufficient protection offered by PH. Nevertheless, EPH and PPH exhibit extremely low contents of both Cl and O indicating their excellent ability to protect the MS surface. Similarly, the inhibition behaviour can be evaluated by Fe content whereas high value of Fe content is commonly correlated to better inhibition behavior (Shafiee *et al*., 2015). In uninhibited solution, MS was severely corroded giving very low value of Fe content. Opportunely, the studied inhibitors give significantly high content of Fe indicating the MS surfaces are less corroded. The inhibitive action of the studied inhibitors follows this order: PPH>EPH>PH.

The inhibition properties of PH, EPH and PPH against the corrosion of MS in 1 M hydrochloric acid can be explained according to the number of adsorption sites and mode of interaction with the metal surface. Inhibitive action of PH is associated with the lone pair of electrons that are available to be shared with metal to form dative bond. Apart from it, PH may be protonated in 1 M HCl solution forming positively charged molecule and interacts with negatively charged metal surface by weak interaction or also called physisorption. The presence of C=N in the molecules of EPH and PPH resulted in stronger adsorption through unoccupied π-orbital that allows donation of electrons from the metal *d*-orbitals to inhibitors as well as sharing of lone pair electrons with metal to form dative bond. The phenyl group that contains π-orbitals in the

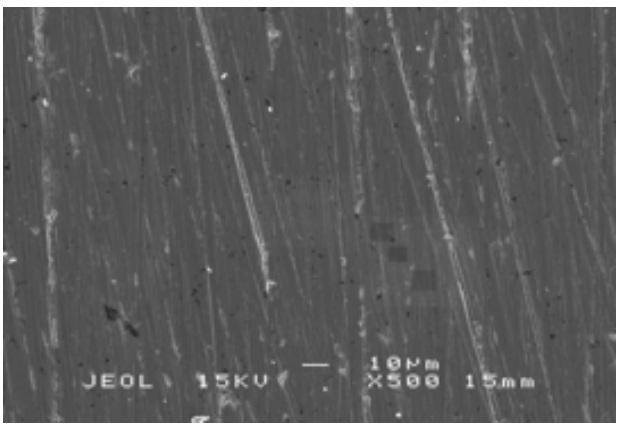

a) Freshly polished MS

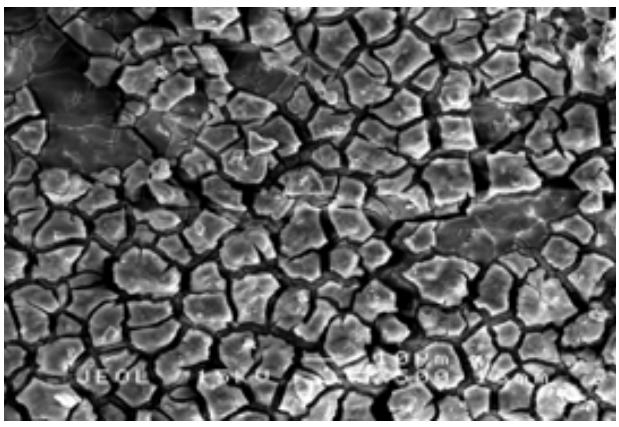

a) Uninhibited 1 M HCl / 30 days (control)

Figure 8. The scanning electron microscopy (SEM) micrographs of freshly polished mild steel surface (a) and mild steel after 30 days of immersion in 1 M HCl (b) at room temperature under 500X magnification.

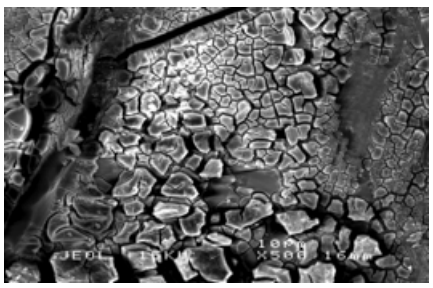

a) PH/30 days

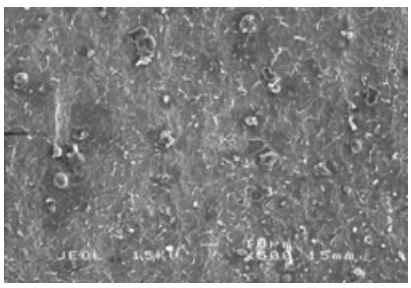

b) EPH/30 days

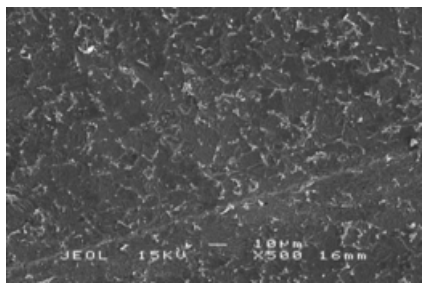

c) PPH/30 days

Figure 9. The scanning electron microscopy (SEM) micrographs of mild steel surface after 30 days of immersion in 1 M HCl in the presence of 200 mg litre^{-1} (a) palmitate hydrazide (PH), (b) N-ethylidene palmitate hydrazide (EPH) and (c) N-*phenylmethylidene palmitate hydrazide (PPH) at room temperature under 500X magnification.*

molecule of PPH enhanced its adsorption on MS surface thus giving excellent inhibition.

CONCLUSION

Corrosion inhibition properties of fatty acid derivatives: PH, EPH and PPH were investigated on MS in 1 M HCl solution using electrochemical measurements. These inhibitors show appreciable inhibitive action to MS surface in the test medium. Nonetheless, EPH and PPH inhibitors exhibit better inhibition properties than PH and their inhibition characteristics follow this order: PPH>EPH>PH. The imines in PPH and EPH molecules allow greater adsorption on the MS surface. The phenyl substituent acts as an additional active centre that enables PPH to exhibit relatively stronger adsorption than EPH. The inhibition efficiency (η%) also increases proportionally to the inhibitor concentration and temperature; and these inhibitors act as mixed-typed inhibitors. Thermodynamic parameter values of free energy of adsorption (ΔG_{ads}) indicate that the inhibitor molecules adsorbed on MS surface through chemisorption accompanied by physisorption. The negative values of ΔG_{ads} reveal that the adsorption is spontaneous and obeys Langmuir isotherm. SEM and EDX analyses confirm the formation of film layer for MS that were immersed in the test solution containing 200 mg litre^{-1} of EPH and PPH.

ACKNOWLEDGEMENT

The authors are very indebted to MPOB for financial support.

REFERENCES

ABDULWALI, N; ENNAJIH, H; ABDALLAH GUENBOUR; ABDELKBIRBELLAOUCHOU; AL SUBARI, R; ANTON, J G and ELMOKHTARESSASSI (2013). Inhibition of mild steel corrosion in 1 M hydrochloric acid by benzimidazolium bromide derivatives. *Aust. J. Basic & Appl. Sci.,7(6)*: 1-8.

ALAM, M; ALOK, R; RAY, A R; ASHRAF; SHARIF, S M and AHMAD, S (2009). Synthesis, characterization and performance of amine modified linseed oil fatty amide coating. *J. Amer. Oil Chem. Soc., 86(6)*: 573–580. DOI: 10.1007/s11746-009-1375-1376.

ASHASSI-SORKHABI, H; GHALEBSAZ-JEDDI, N; HASHEMZADEH, F and JAHANI,

H (2006). Corrosion inhibition of carbon steel in hydrochloric acid by some polyethylene glycols. *Electrochim. Acta, 51(18)*: 3848-3854. DOI: 10.1016/j.electacta.2005.11.002.

BAHRAMI, M J and HOSSEINI, S M A (2012). Electrochemical and thermodynamic investigation of the corrosion behavior of mild steel in 1 M HCl solution containing organic compounds. *Int. J. Ind. Chem., 3*: 30. DOI: 10.1186/2228-5547-3-30.

BENTISS, F; LEBRINI, M and LAGRENCE, M (2005). Thermodynamic characterization of metal dissolution and inhibitor adsorption processes in mild steel/2,5-bis(n-thienyl)-1,3,4-thiadiazoles/hydrochloric acid system. *Corros. Sci., 47(12)*: 2915-2931.

BENTISS, F; LEBRINI, M; VEZIN, H; CHAI, F; TRAISNEL, M and LAGRENÉ, M (2009). Enhanced corrosion resistance of carbon steel in normal sulfuric acid medium by some macrocyclic polyether compounds containing a 1,3,4-thiadiazole moiety: AC impedance and computational studies. *Corros. Sci., 51(9)*: 2165–2173. DOI: 10.1016/j.corsci.2009.05.049.

BOUKLAH, M; HAMMOUTI, B; LAGRENEE, M and BENTISS, F (2006). Thermodynamic properties of 2,5-bis(4-methoxyphenyl)-1,3,4-oxadiazole as a corrosion inhibitor for mild steel in normal sulfuric acid medium. *Corros. Sci., 48*: 2831-2842. DOI: 10.1016/j.corsci.2005.08.019.

CHEN, H J; HONG, T and JEPSON, W P (2000). High temperature corrosion inhibition performance of imidazoline and amide. *Corrosion 2000*. NACE International 2000, USA. Paper No: 35. http://www.corrosioncenter.ohiou.edu/documents/publications/8121.pdf., accessed in February 2016.

DAVIS, J R (2000). *Corrosion: Understanding the Basics*. ASM International, Ohio. p.196.

DESAI, M N; DESAI, M B; SHAH, C B and DESAI, S M (1986). Schiff bases as corrosion inhibitors for mild steel in hydrochloric acid solutions. *Corros. Sci., 26(10)*: 827-837. DOI: 10.1016/0010-938X(86)90066-1.

DURNIE, W; DE MARCO, R; JEFFERSON, A and KINSELLA, B (1999). Development of a structure-Activity relationship for oil field corrosion inhibitors. *J. Electrochem. Soc., 146*: 1751-1756.

EL-LATEEF, H M A (2015). Experimental and computational investigation on the corrosion inhibition characteristics of mild steel by some novel synthesized imines in hydrochloric acid solutions. *Corros. Sci., 92*: 104-117.

EL-MAKSOUD, S A A (2008). The effect of organic compounds on the electrochemical behaviour of steel in acidic media. A review. *Int. J. Electrochem. Sci., 3*: 528-555.

ELAZZOUZIA, M; AOUNITIA, A; TIGHADOUINA, S; ELMSELLEMA, H; RADIA, S; HAMMOUTIA, B; EL ASSYRYB, A; BENTISS, F and ZARROUK, A (2016). Some hydrazine derivatives as corrosion inhibitors for mild steel in 1.0 M HCl: weight loss, electrochemical, SEM and theoretical studies. *J. Mol. Liq., 221*: 633-641.

FOO, K Y and HAMEED, B H (2010). Insights into the modeling of adsorption isotherm systems. *Chem. Eng. J., 156(1)*: 2-10. DOI: 10.1016/j.cej.2009.09.013.

HOSSEINI, M G; MERTENS, S; GHORBANI, M and ARSHADI, M R (2003). Asymmetrical Schiff bases as inhibitors of mild steel corrosion in sulphuric acid media. *Mater. Chem. Phys., 78*: 800-808.

KARTHIKAISELVI, R and SUBHASHINI, S (2014). Study of adsorption properties and inhibition of mild steel corrosion in hydrochloric acid media by water soluble composite poly(vinyl alcohol-o-methoxy aniline). *J. Assn. Arab Univ. Basic Appl. Sci., 16*: 74-82. DOI: 10.1016/j.jaubas.2013.06.002.

KELES, H; EMIR, D M and KELES, M (2015). A comparative study of the corrosion inhibition of low carbon steel in HCl solution by an imine compound and its cobalt complex. *Corros. Sci., 101*: 19-31. DOI: 10.1016/j.corsci.2015.07.013.

KHADIRI, A; SADDIK, R; BEKKOUCHE, K; AOUNITI, A; HAMMOUTI, B; BENCHAT, N; SOLMAZ, R and BOUACHRINE, M (2016). Gravimetric, electrochemical and quantum chemical studies of some pyridazine derivatives as corrosion inhibitors for mild steel in 1 M HCl solution. *J. Taiwan Inst. Chem. Eng., 58*: 552-564. DOI: 10.1016/j.jtice.2015.06.031.

LEBRINI, M; BENTISS, F; VEZIN, H and LAGRENEE, M (2006). The inhibition of mild steel corrosion in acidic solutions by 2,5-bis(4-pyridyl)-1,3,4-thiadiazole: structure–activity correlation. *Corros. Sci., 48(5)*: 1279-1291.

MADKOUR, L H and ELROBY, S K (2014). Correlation between corrosion inhibitive effect and quantum molecular structure of Schiff bases for iron in acidic and alkaline media. *Sci. Res. Essays, 2(13)*: 680-704.

MADKOUR, L H and ELROBY, S K (2015). Inhibitive properties, thermodynamic, kinetics and quantum chemical calculations of polydentate Schiff base

compounds as corrosion inhibitors for iron in acidic and alkaline media. *Int. J. Ind. Chem., 6(3)*: 165-184. DOI: 10.1007/s40090-015-0039-7.

MIGAHED, M A; ABD-EL-RAOUF, M; AL-SABAGH, A M and ABD-EL-BARY, H M (2006). Corrosion inhibition of carbon steel in acid chloride solution using ethoxylated fatty alkylamine surfactants. *J. Appl. Electrochem., 36(4)*: 395-402. DOI: 10.1007/s10800-005-9094-7.

MIKSIC, B A; FURMAN, A Y; KHARSHAN, M A and BOUTELLE, L (2006). Oil-based additive for corrosion inhibitors. United States patent 7014694 B1.

MOHD, N K; YEONG, S K; IBRAHIM, N A and NOOR, S M M (2014). Method to prepare hydrazone from hydrazide. Malaysian patent PI 2014003628.

MONK, K A (2015). Quaternary fatty acid esters as corrosion inhibitors. United States patent 20150240365.

NEGM, N A; GHUIBA, F M and TAWFIK, S M (2011). Novel isoxazolium cationic Schiff base compounds as corrosion inhibitors for carbon steel in hydrochloric acid. *Corros. Sci., 53*: 3566-3575. DOI: 10.1016/j.corsci.2011.06.029.

ÖZCAN, M; KARADAG, F and DEHRI, I (2008). Investigation of adsorption characteristics of methionine at mild steel/sulfuric acid interface: an experimental and theoretical study. *Colloids Surf. A, Physicochem. Eng. Asp., 316*: 55-61.

PALOU, R M; OLIVARES-XOMELT, O and LIKHANOVA, N V (2014). Chapter 19: Environmentally friendly corrosion inhibitors. INTECH Publication. http://dx.doi.org/10.5772/57252, accessed in August 2016.

QURAISHI, M A; JAMAL, D and SAEED, M T (2000). Fatty acid derivatives as corrosion inhibitors for mild steel and oil-well tubular steel in 15% boiling hydrochloric acid. *J. Amer. Oil Chem. Soc., 77*: 265-268.

RAFIQUEE, M Z A; SAXENA, N; KHAN, S and QURAISHI, M A (2007). Some fatty acid oxadiazoles for corrosion inhibition of mild steel in HCl. *Indian J. Chem. Technol., 14*: 576-583.

RAJA, P B and SETHURAMAN, M G (2008). Natural products as corrosion inhibitors for metals in corrosive media: a review. *Mater. Lett., 62(1)*: 113-116. DOI: 10.1016/j.matlet.2007.04.079.

RAMYA, K; MOHAN, R; ANUPAMA, K K and JOSEPH, A (2015). Electrochemical and theoretical studies on the synergistic interaction and corrosion inhibition of alkyl benzimidazoles and thiosemicarbazide pair on mild steel in hydrochloric acid. *Mater. Chem. Phys., 149-150*: 632-647. DOI: 10.1016/j.matchemphys.2014.11.020.

ROILA, A; SALMIAH, A and RAZMAH, G (2001). Properties of sodium soap derived from palm-based dihydroxystearic acid. *J. Oil Palm Res. Vol. 13(2)*: 33-38.

SHAFIEE, S R M; ASHRI, A; ZULKAFLI, M Y: OTHMAN, N K and LAZIM, A M (2015). Effect of red palm oil as a natural corrosion inhibitor toward carbon steel and mild steel in 1 M of hydrochloric acid solution. *Malaysian J. Analytical Sciences, 19*: 679 - 691.

SOLMAZ, R; KARDAS, G; CULHA, M; YAZICI, B and ERBIL, M (2008). Investigation of adsorption and inhibitive effect of 2-mercaptothiazoline on corrosion of mild steel in hydrochloric acid media. *Electrochim. Acta, 53(20):* 5941–5952. DOI: 10.1016/j.electacta.2008.03.055.

TIU, B D B and ADVINCULA, R C (2015). Polymeric corrosion inhibitors for the oil and gas industry: design principles and mechanism. *React. Funct. Polym., 95*: 25-45. DOI: 10.1016/j.reactfunctpolym.2015.08.006.

TARMIZI, A H A; SIEW, W L and KUNTOM, A (2008). Quality assessment of palm products upon prolonged heat treatment. *J. Oleo Sci., 57(12)*: 639-648.

VERMA, C B and QURAISHI, M A (2014). Schiff's bases of glutamic acid and aldehydes as green corrosion inhibitor for mild steel: weight-loss, electrochemical and surface analysis. *Int. J. Innov. Res. Sci. Eng. Technol., 3(7)*: 14601-14613.